International Journal of Advanced Research and Review

www.ijarr.in

# SINGLE-PHASE GRID-CONNECTED PHOTOVOLTAIC SYSTEMS WITH DYNAMIC VOLTAGE SUPPORT FOR LOW-VOLTAGE RIDE-THROUGH OPERATION

[1]R.S.R.Krishnam naidu, [2]V.Pavan kumar, [3] N.Sai Venkat Narisimha, [4]MD.Ariff, [5] M.Surya Teja,

[6]V.Charandev, [7] S.P.Bharath kumar.

[1] Professor, Dept. of EEE, NSRIT, Visakhapatnam, AP

[2,3,4,5,6,7] B. Tech Students, Dept. of EEE, NSRIT, Visakhapatnam, AP

NSRIT-Nadimpalli Satyanarayana Raju Institute of Technology

Abstract

The article introduces a dynamic voltage support (DVS) scheme designed to achieve low-voltage ride-through (LVRT) with a grid-connected photovoltaic (PV) inverter during voltage sag faults. The DVS scheme involves the development of an additional reactive active current control mode, derived from a conventional reactive current control approach, to ensure stable system operation and improved effectiveness, particularly in low-voltage networks with lower X/R ratios at the point of common coupling. The performance of the proposed controller is evaluated through simulations of a 4 kW system for voltage sag faults and further validated through real-time simulations and experimental setups. The results demonstrate that the active and reactive power are regulated in compliance with grid code requirements, enabling the controller to achieve LVRT within the time limits of grid standards during symmetrical faults, making it suitable for fast transient events. This allows the PV system to operate under its nominal capacity, thereby avoiding undesirable grid disconnection events.

Index Terms—Dynamic voltage support (DVS), low-voltage ride-through (LVRT), reactive power control, single-phase grid connected photovoltaic (PV) system.

## I. INTRODUCTION

With the in crease in grid integration of renewable energy over the years, power saturation has been an issue with the grid. The emergence of photovoltaic (PV) power and its intermittent nature is considered to be amaj or contribution to this issue [1]. Further, the integration of smaller PV generations into the grid brings different challenges affecting the grid stability that need to be tackled, especially at the distribution level [2]. Most impacts of grid integrated PV systems are related to un intentional islanding, overloading of feeders, and power quality issues due to unbalanced voltage, dc injection, and flickering [2].

A set of rules has been developed in response to these PV impacts in order to preserve system stability, keep operations within safe bounds, and guarantee grid security [3], [4]. These technical requirements were first placed on wind power systems linked to high-voltage transmission grids, but in recent years, medium- and low-voltage (LV) units that are being connected to the power network have also been subject to them.

PV systems may trip in grid failure scenarios, such as voltage sags, to shield the PV inverters' power electronics components from harm. Therefore, grid rules include stringent criteria on the immunity of the unit to survive these occurrences in order to prevent grid instability brought on by production units tripping in large quantities during fault circumstances.A power converter's internal oscillator has to be tuned in order to maintain synchronisation with the grid and meet the grid's dynamics [5]. Grid synchronisation techniques can be used to ride the system through grid voltage sags since the parameters often employed to meet this objective are the grid voltage and the frequency. Efficient voltage dip detection and precise synchronisation techniques are critical components that enhance the overall control system's dynamic performance and stability margin.
In order to offer a comprehensive variety of ancillary services, such as grid support for PV inverters during grid failures and low-voltage ride-through (LVRT), tive power injection was suggested. To accomplish fault ride-through (FRT) capabilities, the PV characteristics and positive-negative control systems are also covered in [9]. Furthermore, the overload capacity of grid-tied inverters is employed to further strengthen the FRT scheme's supremacy. Typically, these techniques mix external limiters and saturation units with the voltage and current control loops, causing unwanted oscillations and voltage instability. As stated in [10] and [11],

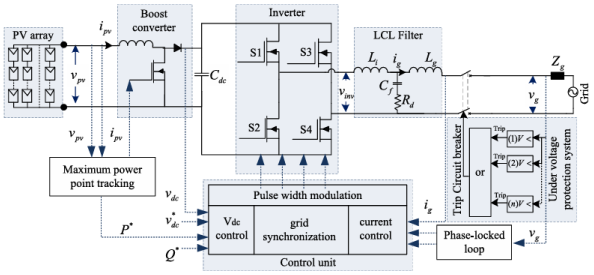


**Fig. 1. Two-stage single-phase grid-connected photovoltaic system with control unit.**

Given the significance of voltage stability in distributed systems, rooftop PV systems are able to accomplish dynamic voltage support (DVS) and LVRT. Additionally, the authors in [11] determined how inverter design margins affected the voltage stability in the near term and created a novel DVS approach [12]. The devised approach makes use of the PV inverters' maximum permitted current in order to obtain active power support from the PV units. According to [13], local reactive power/voltage and plant-level voltage are coordinated to improve short-term voltage stability and fault-induced delayed voltage recovery in a PV system.

The approaches that were previously explored mostly focused on provide reactive and active power support during symmetrical faults. A smart LVRT controller is created in [14] by determining the PV power and current characteristics and synchronising the ride-through controller and maximum power point tracking (MPPT) functions. In order to provide active and reactive power injection control during severe failures, a peak current limiter is presented here. Additionally, employing the grid voltage as a feedforward signal, intelligent power injection techniques [16] and learning-based approaches [15] were used to develop smart inverters.

were created by feeding forward signals derived from the grid voltage. Although these expects have shown to enhance the current controller's performance, they may have measurement delays that compromise the stability of the inverter's operation. In addition to the tactics mentioned above, there is literature on sliding mode control [18] and model predictive power control [17] based voltage support capabilities for grid-connected systems. These control strategies conflict with the discrete character of the power electronics converter and respond slowly. They are also less flexible.

Given the aforementioned problems, this study highlights the challenge of managing a high X/R ratio in LV networks and offering DVS to grid-connected PV systems (GCPVS) in order to achieve LVRT/FRT in the literature. An extra reactive active current control (ARACC) mode is developed to accomplish the DVS in order to address the concerns that have been observed. The traditional reactive current control (RCC) technique, which is frequently employed with systems with a low X/R ratio, provides the basis for the development of the ARACC

method [19], [20]. Reactive current injection into the network with the inclusion of a reactive current component was the traditional method used by the RCC mode to accomplish LVRT during grid disturbances. The ARACC operates similarly in the suggested fashion, but it makes use of an extra active current component.

This helps in the following situations: 1) giving DVS to LV networks with a high X/R ratio; 2) enhancing the grid-connected system's performance by taking the power system network's short-term dynamics into account; and 3) achieving efficient LVRT operation without any system transients and within the grid standards' time constraints.

Moreover, a general two-stage single-phase GCPVS is developed to accomplish these goals. The following provides specifics on the creation and use of the suggested control: The GCPVS control is explained in Section II. An outline of pertinent PV system control modes is provided in Section III, along with a discussion of the creation of the suggested reactive power injection technique. Section V concludes with the findings of the simulation, real-time control, and experimental analysis using the suggested controller that were presented in Section IV.

## II GRID-LINKED SYSTEM MANAGEMENT

The general design of the two-stage single-phase GCPVS is shown here, together with the control settings.Figure 1.Because the boost converter increases the configuration's versatility, it provides the benefit of active power regulation in low solar irradiation situations. An MPPT control strategy based on perturbation and observation is used to provide boost converter control [21]. A dual-loop cascaded controller is used to regulate the inverter; with this controller, the dc link voltage While the inner loop of the controller functions as a current controller, the outer loop controls the voltage differential current. The outer loop, which consists of a feedforward power obtained through panels (Ppv), uses a proportional integrator (PI)-based controller, while the inner loop current controller generates the i∗ g reference using PQ-based theory [6]. This study uses the synchronous reference framephase-locked loop (SRF-PLL), as described in [22], to achieve grid synchronisation. This approach operates on the premise of changing the current variables in a synchronously rotating DQ frame, first processing the voltage signals to obtain the unit vectors. Additionally, the corresponding compensated variables are changed back from the dq frame into the current controller once the transformed current variables are compensated using filters. An effective synchronisation with strong immunity to voltage and current harmonics as well as other power quality imbalances is provided by the SRF-PLL technique. In addition, the switching pulse production process is integrated with the current controller's output to facilitate the functioning of inverter switches. This eliminates the intermittent power output issue with standalone PV systems and improves the inverter's dynamic voltage control capacity. This was made possible by the PV system running in the grid-feeding/grid-supporting mode, which provided a steady and regulated power supply. Additionally, a low pass filter adaptation is required in order to get the fundamental frequency output from the inverter [23]. Third-order LCL filters are typically used in grid-connected and freestanding systems due to its large attenuation value, which extends beyond the resonant frequency. The design requirements for an LCL filter are taken from [24] and include a number of characteristics, including filter resonance and current ripple across the inductor.

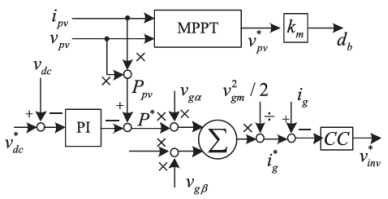


**Fig. 2. Inverter control structure with the current controller.**

$$G_{\mathrm{PI}}(s) = k_p + \frac{k_i}{s} \qquad (1)$$

$$v_{\mathrm{gm}} = \sqrt{v_{g\alpha}^2 + v_{g\beta}^2} \qquad (2)$$

The PI controller (GPI(s)) may be used to regulate the dc link voltage in the following expression: where ki stands for integral controller gain and kp for proportional controller gain. Further, it can be observed from Fig. 2 that vgα

= vg, the grid voltage vg is in the same quadrant as virtual voltage vgβ, so where grid voltage amplitude is indicated by vgm.

The current controller is based on a proportional-resonant (PR) controller [5], which can follow a sinusoidal reference signal at the resonant frequency without incurring any steady-state error. It is accomplished because there is a large gain in the PR controller around the resonance frequency [5]. The transfer function for the inverter is calculated using the sample and the delay added for the pulsewidth modulation generator [5]. The grid voltage differential between the inverter output and grid voltage is sent into the grid filter transfer function, which produces grid feedback current, an input to the PR controller. In the study that is being reported, harmonic compensation is achieved by combining a repeating controller with a PR controller [25].

The current controller's expression may be expressed as follows: PRcontroller, a basic frequency controller, is represented by GPR(s). GRC is the abbreviation for the repetitive controller (s). The PR controller's resonant control gain is shown by kir, while kpr presents the proportional control gain. W0 represents the fundamental grid frequency; krc indicates the RC controller gain; and T0 = 2π/ω0 represents the fundamental period. The low pass filter Q(s) and the phase-lead compensator Gf(s)=esTc, which has a compensation time Tc, are parameters that improve the robustness of the controller [26].

$$G_{cc}(s) = G_{PR}(s) + G_{RC}(s) = k_{pr} + \frac{k_{ir}}{s^2 + w_0^2} + \frac{k_{rc} Q(s) e^{-sT_0}}{1 - Q(s) e^{-sT_0}} . G_f(s) \quad (3)$$

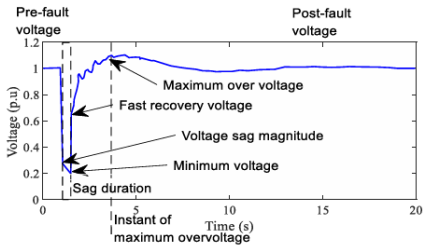


**Fig. 3. Characteristics of fault induced voltage sag.**

III. FAULT RIDE-THROUGH CONTROL

The pertinent GCPV operating modes that affect power system stability—namely, fault-induced delayed voltage recovery and short-term voltage stability—are listed in this section. These control modes often refer to LVRT and DVS capabilities, which specify cutting-edge specifications and configurations in accordance with global standards and grid codes. The main objective is to take into account control modes, namely voltage control modes that affect short-term voltage dynamics.Three distinct control modes are taken into consideration for the PV system's reaction to grid problems, particularly voltage sag.

No LVRT Capability (No LVRT): This mode makes use of the PV plant's undervoltage safety technology, as seen in Fig.

1. In this scenario, the PV inverter separates from the grid if the voltage fluctuates within ±6% of the nominal voltage for longer than the allotted two seconds [27], [28]. Fig. 1 shows the protective relay under consideration. The voltage restrictions and time delays are specified in the undervoltage protection function using the rms values that are extracted from the momentary values. The OR function receives the tripping signal and uses it to open the circuit breaker and disconnect the PV plant.

LVRT and Blocking Mode: This control mode takes into account the PV's blocking ability as well as its LVRT. The PV system's capacity to stay connected to the grid during voltage sag is facilitated by its LVRT capabilities, or more broadly, its FRT capability. Fig. 3 displays the LVRT feature that is being investigated.

The PV system must remain connected to the grid and ride through the fault if the voltage throughout the fault-on time is within the no-trip region. However, if the voltage falls below the LVRT characteristic, the PV system could disconnect. As seen in Fig. 1, a stepwise under-voltage protection system with n functions may be used in practice to provide the LVRT capabilities. The way that active and reactive current behaves during the fault-on

time is the second feature of this control method. Blocking, in this regard, indicates that the PV system does not function in grid feeding or supporting mode throughout the fault-on duration. In the literature, this is also referred to as the zero power mode or the brief cessation mode and is used with several inverters [29].

DVS: Also referred to as dynamic reactive power support or dynamic voltage control, this control mode feature provides voltage support during a disturbance. As seen in Fig. 4, the DVS capability defines an extra reactive current injection that is proportionate to the voltage deviation. The themes that connect with RCC are as follows:

$$I_{\mathrm{Flt}} = \bar{I}_0 + \Delta I\left(\Delta V\right) = I_{d,\mathrm{Flt}} + \mathrm{j}I_{q,\mathrm{Flt}} \qquad (4)$$

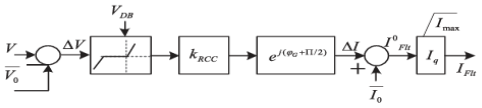


**Fig.4. Dynamic voltage support through reactive current control mode.**

where Id, Flt, and Iq, Flt are the direct and quadratic axis current phasor magnitudes during fault mode, respectively; ΔI is additional current injection during fault mode; ΔV is voltage deviation from prefault value; and I0 is the prefaults current phasor magnitude.

Further,

$$\Delta I\left(\Delta V\right) = e^{\mathrm{j}\left(\phi_{\mathrm{G}}+\frac{\Pi}{2}\right)} \cdot \begin{cases} 0, |\Delta V| \le V_{\mathrm{DB}} \\ k_{\mathrm{RCC}} \cdot \left[\Delta V \mp V_{\mathrm{DB}}\right], |\Delta V| > V_{\mathrm{DB}} \end{cases} \qquad (5)$$

where VDBis voltage-gated edge band for quick voltage control, φ G is the voltage angle of grid equivalent, and kRCC is the controller gain for RCC

$$\Delta V = V - \bar{V}_0 \qquad (6)$$

where V0 is the average voltage phasor value and V is the voltage.

$$\bar{I}_0 = \frac{1}{T}\int_{t'-T}^{t} I\left(t'\right) dt' \qquad (7)$$

where is the current phase and with current restriction, and is the time constant, time in [s], and time in p.u.

$$\bar{V}_0 = \frac{1}{T}\int_{t'-T}^{t} V\left(t'\right) dt' \qquad (8)$$

$$I_{q,\mathrm{Flt}} = \bar{I}_{q,0} + \Delta I_q = \overset{I_{\max}}{\min}\left(\bar{I}_{q,0} + k_{\mathrm{RCC}} \cdot \left[\left(\Delta V\right) \mp V_{\mathrm{DB}}\right]\right) \qquad (9)$$

where Imaxis the maximum current, ΔIq is the change in the value of the quadratic axis current component, and Iq is the quadratic axis current phase or magnitude during the prefault mode.

$$= \begin{cases} 0, & \text{for } i_{\mathrm{FRT\_CI\_PRIO\_MOD}} = 0 \\ \overset{I^0_{\max}}{\min}\left(I_{\max} - I_{q,\mathrm{Flt}}\right), & \text{for} i_{\mathrm{FRT\_CI\_PRIO\_MOD}} = 1 \\ \overset{I^0_{\max}}{\min}\left(\sqrt{\left(I_{\max}\right)^2 - \left(I_{q,\mathrm{Flt}}\right)^2}\right), & \text{for } i_{\mathrm{FRT\_CI\_PRIO\_MOD}} = 2 \end{cases} \qquad (10)$$

where the current priority mode is iFRT_CI_PRIO_MOD: where vpv is the PV system's voltage output and iFRT_CI_STAB is enhanced stability during fault by voltage dependant ID reduction:0=no;1=yes. 1= arithmetic(abs), 2=geometric(sqrt), and other setother value to zero.

$$I^0_{\max} = \begin{cases} I_{\max}, & \text{for } i_{\mathrm{FRT\_CI\_STAB}} = 0 \\ \bar{I}_{d,0} \cdot \left(v_{\mathrm{pv}}\right)^2, & \text{for } i_{\mathrm{FRT\_CI\_STAB}} = 1 \end{cases} \qquad (11)$$

**Fig.5. Dynamic voltage support through additional reactive and active current control mode.**

Adjusting the impedance angle at the PCC allows the PVinverter to inject extra reactive and active current (ARAC), which is the last fault control option.Fig. 5 shows the block representation for the suggested method of operation.Thematics relating to reactive and active current control are provided in (11).

$$I_{\mathrm{Flt}}^{0} = \bar{I}_{0} + \Delta I\ (\Delta V) = I_{d,\mathrm{Flt}}^{0} + \mathrm{j} I_{q,\mathrm{Flt}}^{0} \quad (12)$$

$$I_{\mathrm{Flt}} = I_{\mathrm{Flt}}^{0} \cdot F_{\max} = I_{d,\mathrm{Flt}} + \mathrm{j} I_{q,\mathrm{Flt}} \quad (13)$$

0 in the superscript indicates an unbounded amount, and Fmax is the current limits scaling factor in the fault control mode.

$$\Delta I\ (\Delta V) = e^{\mathrm{j}(\varphi_{\mathrm{Q}} + \Psi_{\mathrm{ARACC}})} \cdot \begin{cases} 0, & |\Delta V| \le V_{\mathrm{DB}} \\ k_{\mathrm{RACC}} \cdot [\Delta V \mp V_{\mathrm{DB}}], & |\Delta V| > V_{\mathrm{DB}} \end{cases} \quad (14)$$

where RCC is the controller for both RCC and active. Additionally, with the current limitation.

$$I_{q,\mathrm{Flt}} = I_{q,\mathrm{Flt}}^{0} \cdot F_{\max} \quad (15)$$

$$I_{d,\mathrm{Flt}} = I_{d,\mathrm{Flt}}^{0} \cdot F_{\max} \quad (16)$$

$$I_{q,\mathrm{Flt}}^{0} = I_{q,0} + \Delta I_{q} = I_{q,0} + [k_{\mathrm{RACC}} \cdot [\Delta V \mp V_{\mathrm{DB}}] \cdot \sin(\Psi_{\mathrm{ARACC}})] \quad (17)$$

$$I_{d,\mathrm{Flt}}^{0} = I_{d,0} + \Delta I_{d} = I_{d,0} + [k_{\mathrm{RACC}} \cdot [\Delta V \mp V_{\mathrm{DB}}] \cdot \cos(\Psi_{\mathrm{ARACC}})] \quad (18)$$

where

$$I_{d,0}^{0} = \begin{cases} I_{d,0}, & \text{for } i_{\mathrm{FRT\_CI\_STAB}} = 0 \\ I_{d,0} \cdot (V_{\mathrm{DC}})^{2}, & \text{for } i_{\mathrm{FRT\_CI\_STAB}} = 1 \end{cases} \quad (19)$$

$$F_{\max} = \max_{1}\left(\frac{I_{\max}}{|I_{\mathrm{Flt}}^{0}|}\right). \quad (20)$$

For the injected ARAC, the direct and quadrature axes are shown in Fig. 6.Figure shows that when active current is injected during a voltage decrease, the active power does not always rise.Moreover, positive active power injection (S=V*I*=P+jQ= (V*Id−jV*Iq)) is indicated by the active sign convection. Negative reactive power exchange (Iq>0) results in voltage decreases during the prefault current. Positive reactive power exchange (Iq < 0) results in voltage increases during full dynamic network support.

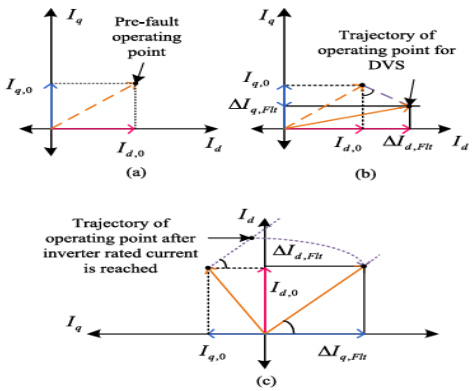


**Fig. 6. Scaling of direct and quadrature axis current in additional reactive and active current control mode.**

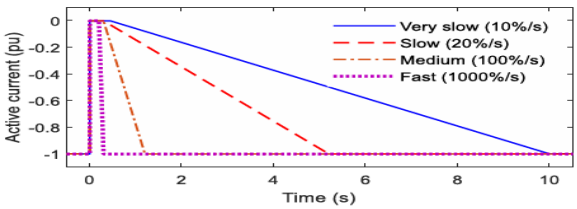


**Fig. 7. Active current recovery rate during the postfault period.**

In addition, the duration until the PV system's active power is recovered following a disturbance is ascertained by measuring the active current recovery rate during the postfault period. The recovery rates under consideration are categorised as extremely slow, moderate, medium, and quick recovery, as seen in Fig. 7. To restore the PV plant's active current during the extremely slow and recovery modes, the recovery rate should be 10%/s and 20%/s, respectively [29].

However, the recovery rate is 100%/s for the medium recovery mode and 100%/s for the rapid recovery option. These figures represent the lowest bounds established for faults lasting longer than 140 ms [30].

IV. RESULTS AND DISCUSSION

Simulation Analysis:

The two-stage single-phase GCPVS simulation in conjunction with to implement the DVS system mentioned in Section III, MATLAB/Simulink 2017b is used. The criteria for design and control
of the system connected to the grid are displayed in Table I.

| System parameter | Value |
|---|---|
| PV array nominal power | 4 $kW$ |
| DC-DC Boost converter | 5 $kHz$, 500 $V$ |
| Boost converter inductance | 10 $mH$ |
| DC link capacitance | 2400 $uF$ |
| DC link Voltage | 400 $V$ |
| Voltage at PCC | 230 $V_{rms}$ |
| Inverter side filter inductance | 2.18 $mH$ |
| Grid side filter inductance | 1 $mH$ |
| Filter capacitance | 2.2 $uF$ |
| DC voltage controller gain | $-12976$ |
| AC voltage controller gain | $-0.5$ |
| Reactive power control gain | $-0.226755$ |
| Reactive power control time constant | 0.002205 $secs$ |
| Gain for ARACC | 6 $p.u.$ |
| Impedance angle at PCC | $90^0$ |

**Table I**

**OVERALL SYSTEM DESCRIPTION FOR 4 KW GCPVS WITH CONTROL PARAMETERS**

A balanced Vrms 230 V ac is considered as the nominal voltage at Vpcc. It is customary to set the dead-band to ± 10\% of the prefault voltage magnitude [1], [2]. The Bureau of Indian Standards' National Electric Code's grid support restrictions serve as the basis for both the modelling and experimental components of the work [31], [32].

The grid code states that the grid-connected PV system must function continuously even in the face of grid anomalies that result in voltage drops in order to operate within predetermined safety limits. By repairing the voltage drop that happened during the grid irregularity, the grid-connected system should be able to regain active power at a quick pace. The time to recovery of the system is 2 s for abnormal grid circumstances that result in a voltage sag variation between 0.5 and 0.9 p.u., and 0.5 s for abnormal grid conditions that result in a voltage sag that falls below 0.5 p.u. The PV system has to be able to cut itself off from the grid's aberrant activity when it reaches this limit.

Additionally, in order to assess the efficacy of the established ARACC technique in meeting the aforementioned objectives, several modes are evaluated by injecting a line to ground (LG) sag fault using design and control parameters that are covered in Table I on the GCPVS.

scenario 1:
A voltage decrease of more than 6% of the nominal voltage is scenario

1.The influence of the LG-sag fault is seen in Fig. 8 at t = 0.2 s, and the VPCC drops from 230 V at steady-state to 200 V. Here, the designed controller causes the current to grow to 18 A and the active power (PPCC) to drop, leading to the rise of reactive power (QPCC). The power at PPCC drops to 2.8 kW as a result of voltage sag, and 1 kV of reactive power is injected to bring the voltage back up.

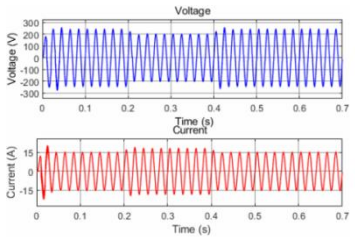


**Fig. 8. Voltage and current at the point of common coupling for voltage drop more than 6%.**

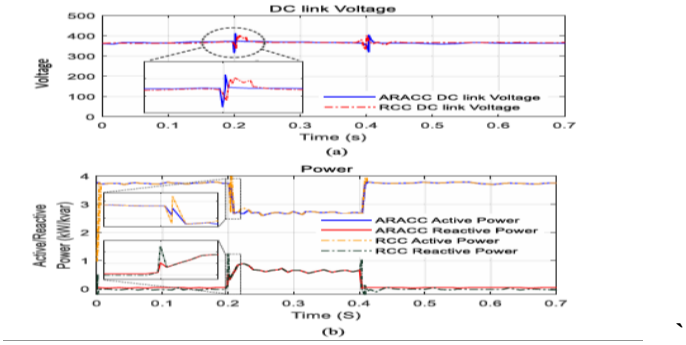


**Fig. 9. CharacteristicsofGCPVwithRCCandARACCforvoltagedropmore than 6%.(a) DC link voltage during voltage sag fault. (b) Active and reactive power during voltage sag.**

The outcomes of RCC and ARACC's combined efforts to attain LVRT are shown in Fig. 9 under simulated conditions. The findings show that there are substantial transients in the dc link voltage, active power, and reactive power during and after the LVRT operation when the system is operated with RCC. These transients lead to the system operating out of balance, which can lead to component or system failure. Furthermore, as needed by FRT regulations, the PV inverter is assisted in riding through the fault by the action of ARACC under the voltage sag circumstances previously discussed. The suggested control strategy acts to clear the issue in 0.2 seconds. Additionally, the active current recovery rate is 100%/s and the dc link voltage is controlled at around 400 Vdc.
Situation 2: A drop in voltage of more than 50% of the normal voltage
In line with the previous scenario, the VPCC drops from a steady-state at t = 0.2 seconds, and the influence of the LG-sag fault is shown. 230 to 110 V, as seen in Figure 10. A reactive power injection of 2.1 kvar is made to restore the voltage when the power at PPCC drops to 1.2 kW due to voltage sag. As seen in Fig. 11, the LVRT is attained using the RCC and ARACC.

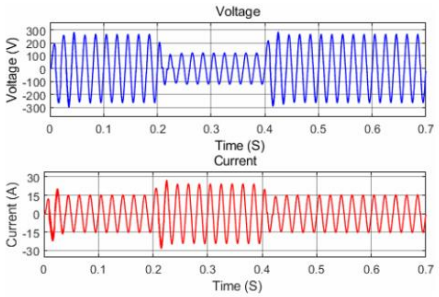


**Fig. 10. Voltage and current at the point of common coupling for voltage drop more than 50%.**

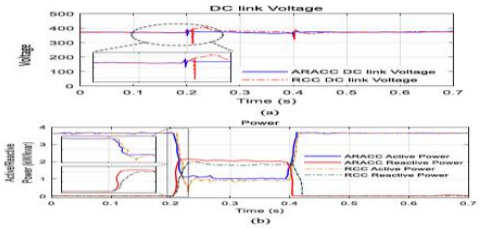


**Fig. 11. Characteristics of GCPV with RCC and ARACC for voltage drop more than 50%.(a) DC link voltage during voltage sag fault (b) Active and reactive power during voltage sag.**

In this case, the reactive power (QPCC) rises while the active power (PPCC) falls, reaching the RCC at 25 A. From the data, it is found that while operating the system with RCC,there are large transients in the dc link voltage, active, and reactive power both during and following the LVRT operation at the time of the voltage sag fault. Additionally, during RCC operation, there were transients in the dc link voltage, which had an effect on the system's active power. These transients lead to an imbalance in the system's functioning, which can lead to component or system failure. Furthermore, in accordance with FRT standards, the ARACCmode assists the PVinvertertoride in overcoming the fault. The suggested control strategy acts to clear the issue in 0.2 seconds.

Moreover, the designed controller operates efficiently since the dc link voltage is controlled at around 400 Vdc and the active current recovery rate is 100%/s.

| System | Parameter | Values |
|---|---|---|
| | Module Characteristics | |
| PV Array Simulator 4 $kWp$ using (Topsun solar 250 $W$ Modules) | Power ($P_{max}$) | 250 $W$ |
| | Short circuit current of the module ($I_{sc}$) | 14.6 $A$ |
| | Open circuit voltage of the module ($V_{oc}$) | 22 $V$ |
| | Maximum power point current ($I_{mpp}$) | 13.9 $A$ |
| | Maximum power point voltage ($V_{mpp}$) | 18 $V$ |
| Inverter Stack (Semikron) [33] | DC bus voltage | 1100 $V_{dc}$ |
| | Maximum continuous output current | 600 $A$ to 1200 $A_{rms}$ |
| | Switching Frequency | 5 $kHz$ |
| | Maximum inverter output voltage | 690 $V_{AC}$ |
| ST microelectronics STGB30NC60K IGBT | Collector emitter voltage | 600 $V$ |
| | Continuous collector current at $25^0C$ temperature | 60 $A$ |
| Fairchild RURP1560 diodes | DC blocking voltage | 600 $V$ |
| | Average rectified forward current | 15 $A$ |
| Grid Simulator | Output power | 30 $kVA$ |
| | Output voltage | 0~300 $V$ |
| | Output frequency | 30 $Hz$ – 100 $Hz$ |

**TABLE II**

**DETAILS OF 4 KWSINGLE-PHASE GRID-CONNECTED SOLAR PHOTOVOLTAIC SYSTEMS EXPERIMENTAL SETUP**

## V. **CONCLUSION**

In order to accomplish LVRT in single-phase GCPVS, this study designed an extra reactive active power control mode for DVS.Ageneric GCPVS models are developed initially.Additionally, the DVS and the active current recovery rate management modes that affect the power system's dynamic performance—more especially, its short-term dynamics—are identified. When a defect is detected, the DVS is accomplished by adding more active and reactive current components to the PCC voltage within the allotted time frame. The suggested controller maintained the PV system's operation at its nominal capacity by preventing unintentional grid disconnection events, controlled active and reactive power, and achieved LVRT within the time constraints of the grid standard for the different voltage sag levels tested during the research.

REFERENCES [1] Y. Wang, B. Ren, and Q.-C. Zhong, “Bounded-voltage power flow control for grid-tied PV systems,” IFAC-PapersOnLine, vol. 50, no. 1, pp. 7699–7704, Jul. 2017.

[2] M. S. ElNozahy and M. M. A. Salama, “Technical impacts of grid connected photovoltaic systems on electrical networks—A review,” J. Renewable Sustain. Energy, vol. 5, no. 3, May 2013, Art. no. 032702.

[3] IEEE Standard for Interconnection and Interoperability of Distributed Energy Resources With Associated Electric Power Systems Interfaces, IEEE STD 1547-2018, 2018.

[4] IEEE Standard for Interconnecting Distributed Resources With Electric Power Systems, IEEE STD 1547, 2003.

[5] R. Teodorescu, M. Liserre, and P. Rodríguez, Grid Converters for Photo voltaic and Wind Systems. Hoboken, NJ, USA: Wiley, 2011.

[6] Y. Yang, F. Blaabjerg, and H. Wang, “Low-voltage ride-through of single phase transformerless photovoltaic inverters,” IEEE Trans. Ind. Appl., vol. 50, no. 3, pp. 1942–1952, May/Jun. 2014.

[7] J. E.-G. Carrasco, J. M. Tena, D. Ugena, J. Alonso-Martinez, D. Santos Martin, and S. Arnaltes, “Testing low voltage ride through capabilities of solar inverters,” Elect. Power Syst. Res., vol. 96, pp. 111–118, Mar. 2013.

[8] Y. Yang, A. Sangwongwanich, H. Liu, and F. Blaabjerg, “Low voltage ride-throughoftwo-stagegrid-connectedphotovoltaicsystemsthroughthe inherent linear power-voltage characteristic,” in Proc. IEEE Appl. Power Electron. Conf. Expo., 2017, pp. 3582–3588.

[9] M.S.ElMoursi, W. Xiao, and J. L. Kirtley, “Fault ride through capability for grid interfacing large scale pv power plants,” IET Gener. Transmiss. Distrib., vol. 7, no. 9, pp. 1027–1036, 2013.

[10] J. Yaghoobi, N. Mithulananthan, and T. K. Saha, “Dynamic voltage sta bility of distribution system with a high penetration of rooftop PV units,” in Proc. IEEE Power Energy Soc. General Meeting, 2015, pp. 1–5.

[11] M. Islam, N. Mithulananthan, and M. J. Hossain, “Dynamic voltage support by TL-PV systems to mitigate short-term voltage instability in residential dN,” IEEE Trans. Power Syst., vol. 33, no. 4, pp. 4360–4370, Jul. 2018.

[12] M. Islam, M. Nadarajah, and M. J. Hossain, “Short-term voltage stability enhancementinresidentialgridwithhighpenetrationofrooftopPVunits,” IEEE Trans. Sustain. Energy, vol. 10, no. 4, pp. 2211–2222, Oct. 2019.

[13] G. Lammert, D. Premm, L. D. P. Ospina, J. C. Boemer, M. Braun, and T. Van Cutsem, “Control of photovoltaic systems for enhanced short-term voltage stability and recovery,” IEEE Trans. Energy Convers., vol. 34, no. 1, pp. 243–254, Mar. 2019.

[14] H. Khan, S. J. Chacko, B. G. Fernandes, and A. Kulkarni, “Reliable and effective ride-throughcontrolleroperationforsmartPVsystemsconnected to LV distribution grid under abnormal voltages,” IEEE J. Emerg. Sel. Topics Power Electron., vol. 8, no. 3, pp. 2371–2384, Sep. 2020.

[15] L. Zhou, A. Swain, and A. Ukil, “Reinforcement learning controllers for enhancement of low voltage ride through capability in hybrid power sys tems,” IEEETrans.Ind.Inform.,vol.16,no.8,pp. 5023–5031,Aug.2020.

[16] H. Alenius, R. Luhtala, T. Messo, and T. Roinila, “Autonomous reactive power support for smart photovoltaic inverter based on real-time grid impedancemeasurementsofaweakgrid,”Elect.PowerSyst.Res.,vol.182, May 2020, Art. no. 106207. [17] Y. Shan, J. Hu, and J. M. Guerrero, “A model predictive power control method for PV and energy storage systems with voltage support capabil ity,” IEEE Trans. Smart Grid, vol. 11, no. 2, pp. 1018–1029, Mar. 2020.

[18] N. Kumar, T. K. Saha, and J. Dey, “Sliding-mode control of PWM dual inverter-based grid-connected PV system: Modeling and performance analysis,” IEEE J. Emerg. Sel. Topics Power Electron., vol. 4, no. 2, pp. 435–444, Jun. 2016.

[19] J.L.GarcíadeVicuña,J.delaHoz,J.Miret,A.Camacho,andM.Castilla, “Reactive current injection protocol for low-power rating distributed gen eration sources under voltage sags,” IET Power Electron., vol. 8, no. 6, pp. 879–886, Jun. 2015.

[20] Y. Yang, H. Wang, and F. Blaabjerg, “Reactive power injection strategies for single-phase photovoltaic systems considering grid requirements,” IEEE Trans. Ind. Appl., vol. 50, no. 6, pp. 4065–4076, Nov./Dec. 2014.

[21] Y. Yang and F. Blaabjerg, “Overview of single-phase grid-connected photovoltaic systems,” Elect. Power Compon. Syst., vol. 43, no. 12, pp. 1352–1363, Jul. 2015.

[22] S.-H.Hwang,L.Liu,H.Li,andJ.-M.Kim,“DCoffseterrorcompensation for synchronous reference frame PLL in single-phase grid-connected converters,” IEEE Trans. Power Electron., vol. 27, no. 8, pp. 3467–3471, Aug. 2012.

[23] M.JayaramanandV.T.Sreedevi,“ImplementationofLCandLCLpassive f ilters for harmonic reduction in PV based renewable energy systems,” in Proc. Nat. Power Electron. Conf., 2017, pp. 363–369.

[24] A. Reznik, M. G. Simoes, A. Al-Durra, and S. M. Muyeen, “LCL filter design and performance analysis for grid-interconnected systems,” IEEE Trans. Ind. Appl., vol. 50, no. 2, pp. 1225–1232, Mar. 2014.

[25] Y. Yang, K. Zhou, H. Wang, F. Blaabjerg, D. Wang, and B. Zhang, “Fre quency adaptive selective harmonic control for grid-connected inverters,” IEEE Trans. Power Electron., vol. 30, no. 7, pp. 3912–3924, Jul. 2015.

[26] F.A.Silva,“Periodiccontrolofpowerelectronicconverters[Booknews],” IEEE Ind. Electron. Mag., vol. 11, no. 2, pp. 71–72, Jun. 2017. [27] M.A.Khan,V.S.BharathKurukuru, A. Haque, and S. Mekhilef, “Island ing classification mechanism for grid-connected photovoltaic systems,” IEEE J. Emerg. Sel. Topics Power Electron., vol. 9, no. 2, pp. 1966–1975, Apr. 2021.

[28] A.Z.Fatama,M.A.Khan,V.S.B.Kurukuru,A.Haque,andF.Blaabjerg, "Coordinated reactive power strategy using static synchronous compen sator for photovoltaic inverters," Int. Trans. Elect. Energy Syst., vol. 30, no. 6, Jun. 2020, Art. no. e12393.

[29] "1200 MW fault induced solar photovoltaic resource interruption distur bance report," North American Electric Reliability Corporation (NERC), 2017, Art. no. 32.

[30] A. Johnson, "Fault ride through RfG- Compliance," Nationalgrid, pp. 1–12, 2014.